BASIC SCIENCE

Nanomedicine: Nanotechnology, Biology, and Medicine
13 (2017) 1663–1671

Original Article

nanomedjournal.com

Direct detection of nano-scale extracellular vesicles derived from inflammation-triggered endothelial cells using surface plasmon resonance

Baharak Hosseinkhani, PhD[a,*], Nynke van den Akker, PhD[d], Jan D'Haen, PhD[b], Mick Gagliardi, BASc[d], Tom Struys, PhD[a], Ivo Lambrichts, PhD[a], Johannes Waltenberger, PhD[e,f], Inge Nelissen, PhD[g], Jef Hooyberghs, PhD[c,g], Daniel G.M. Molin, PhD[d], Luc Michiels, PhD[a,*]

[a]*Hasselt University, Biomedical Research Institute, Hasselt, Belgium*
[b]*Hasselt University, Institute for Materials Research, Hasselt, Belgium*
[c]*Hasselt University, Theoretical Physics, Hasselt, Belgium*
[d]*Maastricht University, Department of Physiology, Cardiovascular Research Institute Maastricht (CARIM), Maastricht, The Netherlands*
[e]*Department of Cardiovascular Medicine, University Hospital Münster, Münster, Germany*
[f]*Cells-in-Motion Cluster of Excellence (EXC 1003—CiM), University of Münster, Münster, Germany*
[g]*Flemish Institute for Technological Research (VITO), Mol, Belgium*

Received 7 December 2016; accepted 19 March 2017

Abstract

A major conceptual breakthrough in cell signaling has been the finding of EV as new biomarker shuttles in body fluids. Now, one of the major challenges in using these nanometer-sized biological entities as diagnostic marker is the development of translational methodologies to profile them. SPR offers a promising label-free and real time platform with a high potential for biomarker detection. Therefore, we aimed to develop a uniform SPR methodology to detect specific surface markers on EV derived from patient with CHD. EVs having an approximate size range between 30 and 100 nm (~48.5%) and 100-300 nm (~51.5%) were successfully isolated. The biomarker profile of EV was verified using immunogold labeling, ELISA and SPR. Using SPR, we demonstrated an increased binding of EV derived from patients with CHD to anti-ICAM-1 antibodies as compared to EV from healthy donors. Our current findings open up novel opportunities for in-depth and label-free investigation of EV.

Key words: Biosensor; Extracellular vesicles; Inflammation; Cardiovascular disease; Endothelial cells; Biomarkers

Cardiovascular disease (CVD) is the number one cause of mortality in EU (with 1.9 million deaths each year) and worldwide.[1] Current epidemiological and clinical studies have shown that many triggers of atherosclerosis and CVD such as smoking, elevated blood sugar, hypertension, diabetes, infection, homocysteine, ischemia and oxidant damage are acting in coordinated or synergistic manner through one or more inflammatory pathways.[2] These observations indicate that

Abbreviations: EV, extracellular vesicles; uEV, extracellular vesicles derived from un-stimulated cells; tEV, extracellular vesicles derived from TNF-α stimulated cells; CVD, cardiovascular disease; CHD, coronary heart disease; ELISA, enzyme-linked immunosorbent assays; SPR, surface plasmon resonance; HUVEC, human umbilical vein endothelial cells; TNFα, tumor necrosis factor alpha.

Conflict of interest disclosure: The authors declare no competing financial interests.

Financial support: This work was co-financed by the EU through the Interreg IV Flanders-the Netherlands project VaRiA (IVA-VLANED-3.65) and Interreg V Flanders–the Netherlands project Trans Tech Diagnostics (TTD) and Johannes Waltenberger is supported by Cells-in-Motion Cluster of Excellence (EXC 1003—CiM), University of Münster, 48149 Münster, Germany.

Prior presentations: The work was presented at the 5th Annual Meeting of the International Society for Extracellular Vesicles in Rotterdam, the Netherlands, 4-7th May 2016.

*Corresponding authors at: Hasselt University, Biomedical Research Institute, Martelarenlaan 42, 3500 Hasselt, Belgium.
E-mail addresses: Baharak.hosseinkhani@uhasselt.be (B. Hosseinkhani), Luc.Michiels@uhasselt.be (L. Michiels).

http://dx.doi.org/10.1016/j.nano.2017.03.010

there is a strong link between inflammation as indicated by associated biomarkers and future CVD events.[2] Moreover, a wide range of functional biomarkers during inflammation are principally transported through biological fluids by secreted nanosized extracellular vesicles (EV) for intercellular communication and autocrine signaling.[3-5] Many studies now appreciate that the cargo of EV is a mirror of the physiological condition of the cell of origin and is tightly linked to the stage of a disease.[6] Hence, profiling of EV-associated inflammation biomarkers as a cell-specific signature holds potential for the next generation of personalized diagnostics.[7,8] Optimistically, EV-based diagnostic tools are expected to become a breakthrough technology for early, less invasive diagnosis of various diseases and effective monitoring of disease progression during therapy including CVD.[9]

Although, conventional methodologies for biomarker discovery such as Western blot analysis and enzyme-linked immunosorbent assays (ELISA) are routinely applied for the qualitative and quantitative assessment of certain disease-related EV biomarkers, these assays require large amounts of sample, long-term processing and extensive post-labeling processes for detection, thus limiting their application in the EV study.[10] Therefore, development of robust profiling techniques for discovering and detecting disease-related EV biomarkers is urgently needed. More recently, the advent of label-free and real-time biosensor platforms has opened a new avenue in profiling of biomarkers with enormous potential in early detection of disease-related biomarkers for more effective treatment and monitoring of disease progression.[11] Unlike conventional optical assays, surface plasmon resonance (SPR)-based biosensors are principally based on measuring optical contrast originating from a change in interfacial refractive index caused by biomolecular adsorption without the need for labels or stains in real time.[12] Although SPR has received extensive interest as one of the latest innovative technologies in medical research, so far relatively few investigations have explored the potential of this technique in the detection and molecular profiling of EV-associated inflammation.[13] We thus sought to develop a label-free SPR-based methodology for biomarker profiling of EV released from cells that cope with inflammatory stress.

In this study, the size distribution and concentration of isolated EV from un-stimulated and from inflamed endothelial cells were investigated using transmission electron microscopy (TEM) and nanoparticle tracking analysis (NTA). In addition, we applied different label-based and label-free methodologies for biomarker profiling and quantifying of isolated EV from inflammation-induced vascular endothelial cells to mimic CVD in patients. Our current findings open up novel opportunities for in-depth and label-free investigation of EV-related biomarkers in a high-end SPR platform.

Methods

Materials

Mouse monoclonal anti-ICAM-1 antibody, exosome CD9 monoclonal antibody (Ts9), exosome CD63 monoclonal antibody (Ts63), exosome CD81 monoclonal antibody (Ts81), gold conjugated goat anti-mouse IgG and anti-rat IgG1 antibody clone (MRG1–58) were obtained from Santa Cruz Biotechnology, Inc. (Heidelberg, Germany), Life Technologies Europe B.V. (Gent, Belgium), AURION (Wageningen, the Netherlands) and BioLegend (San Diego, USA), respectively. 1-Ethyl-3-(3-dimethylaminopropyl) carbodiimide hydrochloride (EDC) and *N*-hydroxysuccinimide were provided by Life Technologies Europe B.V. Sepharose CL-2B and bovine serum albumin (BSA) were purchased from Sigma (Diegem, Belgium).

Cells and culture conditions

Human umbilical vein endothelial cells-2 (HUVEC-2, BD Bioscience, cat. # 354151) at passage 5 were used. Cells were seeded at a density of 600,000 cells in 75 cm^2 cell culture flasks containing endothelial basal medium (EBM-2) (Lonza, Walkersville, MD, USA) supplemented with EGM-2 MV SingleQuot Kit (Lonza, Walkersville, MD, USA) and 5% vesicles-depleted fetal bovine serum (System Bioscience, Mountain View, CA, USA).[14] To simulate a stress response, HUVECs were exposed to 10 ng mL^{-1} TNF-α overnight.[6] All flasks were incubated in a humidified atmosphere condition of 5% CO_2/95% O_2 at 37 °C for 48 h. Afterward, the supernatants were harvested for the isolation of EV. All collected supernatant samples containing EV were stored at −80 °C until EV isolation procedures.

Patient-derived primary vascular endothelial cells

Vascular endothelial cells (VECs) from patients with coronary heart disease (CHD) ($n = 10$) and healthy donors ($n = 6$) were extracted. In short, patients undergoing percutaneous intervention for stable and unstable coronary syndrome were included. The Medical Ethical Committee of Maastricht University (METC nr: M08-1856) and Central Committee on Research involving Human Subject (CCMO-nr: NL24071.060.08) approved the study protocol, and all subjects gave their written informed consent before participating in the study. Blood samples were collected from volunteer patients and healthy individuals in accordance with the WHO guideline on drawing blood. After placement of the arterial sheath, 50 mL of blood was drawn. Mononuclear cells were isolated using Ficoll (PE) gradient centrifugation. Cells were depleted for CD14+ cells using magnetic bead isolation (BD). The remaining fraction was plated in EGM2-MV culture medium (Lonza) and monitored for endothelial outgrowth cells, after which these were sub-cultured. As healthy control cells, commercially available endothelial cells derived from healthy donors were used (human microvascular endothelial cells, human coronary arterial endothelial cells, human coronary microvascular endothelial cells, human saphenous vein endothelial cells (Lonza) and human umbilical vein endothelial cells (BD)). Cells between passages 5 and 9 were used for the experiment. For the experiment, cells were seeded in quadruplicate in wells of a 6 wells plate (Greiner) in a concentration of 10,000 cells/cm^2 in EGM-2MV containing 5% EXO-FBS (Atlas) instead of the regular FBS. Cells were cultured until 75% confluency. Then, medium was refreshed. After 48 h, 2 out of 4 wells were stimulated overnight with 10 ng/mL TNF-α, after which supernatants were collected for further analysis.

Isolation of EV by ultracentrifugation (UCF)

EVs were isolated from cell culture supernatant of un-stimulated (uEV) and TNF-α stimulated (tEV) using differential centrifugation. Briefly, collected supernatant was centrifuged at 300*g* for 5 min to eliminate cell debris. To remove remaining debris, another two centrifugation steps were performed for 10 min and 30 min at 2000 and 10,000*g* respectively. Thereafter, the concentrated supernatant was centrifuged at 110,000*g* for 90 min to pellet the cell-derived EV. All ultracentrifugation steps were performed using an L-90 Beckman centrifuge (Beckman Instruments, Inc., Fullerton, CA, USA) equipped with a Ti-70 rotor (Beckman Instruments) at 4 °C. Pellets were resuspended in 1 mL PBS.[5]

Isolation of EV by size exclusion chromatography (SEC)

EVs from the concentrated supernatant of HUVEC using in-house made size exclusion chromatography columns containing sepharose CL-2B (GE Healthcare, Munich, Germany) were isolated according to the Böing et al.[15] The protein-containing fractions were applied for further analysis.

Isolation of EV using ExoQuick-TC™ (ExoQ)

Isolation of EV from cell culture supernatant of un-stimulated and TNF-α stimulated HUVEC was carried out using commercially available ExoQuick-TC™ precipitation kit (SBI, System Bioscience, Mountain View, CA, USA) according to the supplier's instructions. All purified EVs were stored either at −20 °C for days or kept frozen at −80 °C for weeks.

Total protein concentration of EV

Total protein content of isolated EV was determined using the Micro BCA Protein Assay Reagent Kit (Thermo Scientific Pierce, Rockford, IL, USA)) following the manufacturer's specifications.

Characterization of EV by TEM

Five μL of vesicles pellets was resuspended in PBS and deposited on Formvar–carbon coated EM grids and dried at room temperature. The grids were then transferred into a 50-μL drop of 1% glutaraldehyde for 5 min followed by 5 washing steps in a 50-μL drop of water. Afterward, the fixed vesicles on Formvar–carbon coated copper grids were analyzed using a Tecnai G2 transmission electron microscope (TEM; Tecnai G^2 spirit twin, FEI, Eindhoven, the Netherlands) operated at 120 kV. The microscope was provided with a bottom mounted digital camera FEI Eagle (4k × 4k pixels) to acquire images of the evaluated samples. Digital processing of the images was performed with the FEI imaging software (TEM Imaging & Analysis version 3.2 SP4 build 419.).

NTA analysis of EV

Size distribution and concentration of the isolated EV were analyzed based on the tracking of light scattered by vesicles moving under Brownian motion using the NanoSight NS500 system equipped with a 532-nm laser (NanoSight Ltd., Amesbury, United Kingdom). Samples were introduced into the sample chamber and measured for 60 s at 25 °C with manual shutter and gain adjustments. The data were captured and analyzed using NTA 3.0 software (NanoSight Ltd). Samples were diluted with PBS over a range of concentrations to obtain between 10 and 100 particles per image (optimal ~50 particles per image).[16] Measurements were carried out for 60 s per run, with 3 runs per reading, for 5 individual samples.

TEM analysis of immunogold-labeled EV

Samples for immunogold labeling were prepared by fixation of pellets containing vesicles with 2% paraformaldehyde followed by deposition onto Formvar–carbon coated EM grids. Air dried samples were washed twice with PBS (3 min each) and twice with PBS/50 mM glycine, and finally transferred to a drop of blocking buffer containing PBS/0.5% BSA (10 min). Blocked grids were then incubated with 20 μg/mL antibodies to CD9, CD63, CD81 and ICAM-1 in PBS/0.5% BSA for 30 min. Finally, the grids were washed 5 times with PBS/0.5% BSA for 3 min, incubated with gold-labeled secondary antibody in PBS/0.5% BSA for 30 min, and then washed 5 times for 3 min in 100 μL drops of PBS/0.5% BSA.[17] To detect the cross linking of gold nanoparticles with EVs, a negative control was prepared by omitting the primary antibody from grids and 10 nm colloidal gold conjugated goat anti-mouse IgG was applied as secondary antibody in all samples. TEM analysis was performed with a Tecnai G2 transmission electron microscope as described above.

ICAM-1 ELISA

ELISA was also used to quantify ICAM-1 expression levels on EV-surface and supernatant using the commercially available ICAM-1 Human ELISA Kit (Abcam, Cambridge, UK). All experiments were performed in triplicate. The supernatant of cell-free culture medium supplemented with or without TNF-α served as controls. The wells were only treated with a second antibody served as blank and were subtracted from all corresponding data points.

SPR analysis

Antibodies were immobilized on C1 sensor chip series S according to the standard amine covalent coupling procedures with filtered 1 × HBS-N (0.1 M HEPES, 1.5 M NaCl, pH 7.4) as running buffer. Briefly, surface carboxyl groups were activated using a 1:1 mixture of 1-ethyl-3-(3-dimethylaminopropyl) carbodiimide hydrochloride (EDC) (1 M) and *N*-hydroxysuccinimide (0.25 M). Forty ng/mL of each antibody in 10 mM sodium acetate buffer (pH 4.5) was passed over the activated surface. The residual carboxyl groups were then quenched with 1 M ethanolamine, pH 8.5. After finishing the immobilization procedure, the antibody-immobilized chip was equilibrated with PBS at 25 °C. To determine the affinity of EV to immobilized antibodies, 378 μL of EV was injected into the sensing channels for 2100 s with a flow rate of 10 μL min^{-1}. After subtracting the sensorgram from the control channel, the binding responses of EV to the captured antibodies were obtained. All SPR experiments were monitored using a Biacore T200 optical biosensor (GE Healthcare, Uppsala, Sweden) in PBS as running buffer at 25 °C. Results are expressed as resonance units, RU (one RU is equivalent to one picogram per

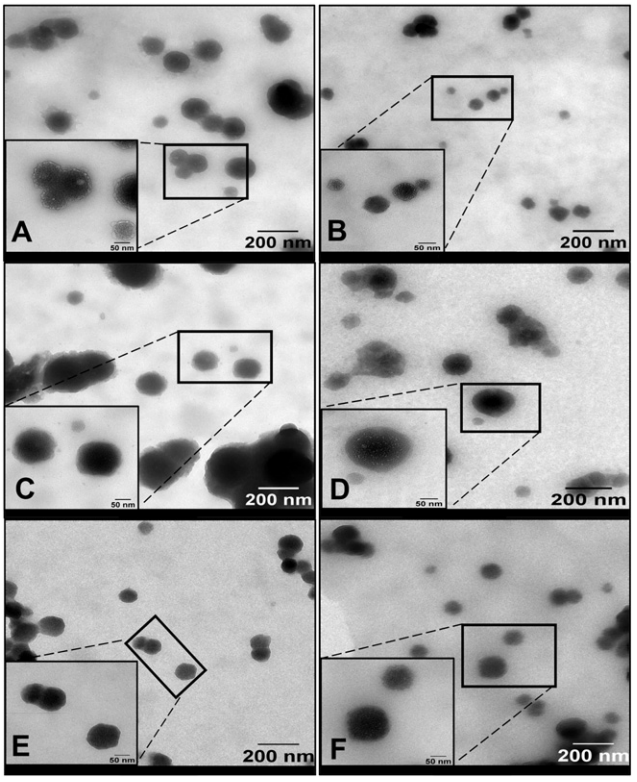

Figure 1. Ultrastructure morphological characterization of EV using TEM. Electron micrographs of isolated EV from the culture supernatant of unstimulated (**A**, **C** and **E**) and stimulated HUVEC with TNF-α (**B**, **D** and **F**) using ExoQ (**A** and **B**), UCF (**C** and **D**) and SEC (**E** and **F**). The corresponding higher magnification TEM micrographs of marked EV within the enclosed area are shown at the insets.

square millimeter on the sensor surface). SPR analysis of all samples was performed in triplicate.

Statistical analysis

The statistical significance between groups was evaluated by one-way analysis of variance (ANOVA) and Student's test using the statistical packages JMP (version pro 12.0; SAS Institute Inc., Cary, NC, USA). Value of $P < 0.05$ was considered as statistically significant. Data were expressed as mean ± standard deviation (SD) of three independent experiments. Using the JMP program, a statistical power analysis was performed (assuming a two-tailed test, $P < 0.05$ and power of 80%) to estimate the minimum number of sample that is needed to discriminate between healthy and patient samples without considering the inflammatory stress.

Results

Isolation, morphological characterization and sizing of EV

EVs were purified from the culture supernatant of HUVEC, either unstimulated (uEV) or stimulated (tEV) with TNF-α to induce an inflammatory stress response. Morphology and size of isolated EV were evaluated by TEM. Electron micrographs revealed that the vesicle-shaped particles were successfully isolated from supernatant of unstimulated (Figure 1, *A*, *C*, *E*) and stimulated HUVEC (Figure 1, *B*, *D*, *F*) using ExoQ (Figure 1, *A*, *B*), UCF (Figure 1, *C*, *D*) and SEC (Figure 1, *E*, *F*). The insets show TEM images of marked EVs with enclosed area at higher magnification.

Next, NTA was applied to measure the size distribution and concentration of uEV and tEV (Table 1). The percentage of EV subpopulation in the size range of exosomes (30-100 nm) and microvesicles (100-300 and >300 nm) (Table 1) was also calculated. Results revealed that EVs having a size range between 30 and 300 nm were successfully isolated from both unstimulated and TNF-α stimulated endothelial cells and the majority of isolated EVs are in the size range of microvesicles (~51.5%) and exosomes (~48.5%) (Table 1).

In addition, results showed that there was a significant condition-depended increase of EV's concentration and size if cells were treated with TNF-α (Table 1). On average, the mean size of tEV isolated using ExoQ and SEC methods was consistently larger than those from uEV. As presented in Table 1, higher concentrations of EV were also detected by NTA in TNF-α stimulated HUVEC (tEV) when compared to non-stressed (unstimulated) cells (uEV). Overall, a difference in the concentration of isolated EV was also noted depending on the isolation procedure. In this regard TEM images of EV in combination with NTA showed that ExoQ and UCF yielded the highest EV concentration values as compared to SEC, but also a more heterogeneous population of EV (Figures 1 and 2).

Screening of biomarkers present on EV surface using targeted immunogold labeling

First, we employed an antigen-specific visualization protocol using ultrastructural immunogold labeling to investigate whether the inflammatory stress has an impact on the expression of classical EV membrane-bound biomarkers including CD9, CD63, CD81 and/or intercellular adhesion molecule-1 (ICAM-1) as a candidate marker of vascular inflammation. A parallel detection and semi-quantitative screening of biomarkers present on uEV and tEV surface was obtained using immunogold-conjugated antibodies against ICAM-1 (Figure 2, *A-D*), CD9 (Figure 2, *E-H*), CD63 (Figure 2, *I-L*), CD81 (Figure 2, *M-P*) and TEM analysis.

In agreement with the results of the NTA analysis, an increase in the number of all sub-populations of tEV (Figure 2, *C*, *G*, *K*, *O*) was observed in comparison with sub-populations of uEV (Figure 2, *A*, *E*, *I*, *M*). Although a positive labeling in the outer layer of all UCF-isolated EV was detected, TNF-α stimulated HUVECs released more ICAM-1(+) and CD63(+) EV than other biomarkers (Figure 2, *C*, *G*, *K* and *O*). Further investigations were focused on these two biomarkers. The same experimental labeling procedure was performed for ExoQ-based isolated EV. In this method, non-specific bindings of gold conjugated secondary antibody as background noise were detected (data not shown). In our study, the UCF method was therefore selected as a further isolation procedure for quick, cost-efficient and routine extraction of EV.

Quantitative assessment of ICAM-1 present on EV-surface and supernatant

Ultrastructural immunogold labeling analysis is only a semi-quantitatively visualization of the ICAM-1(+) EV derived

Table 1
Size distribution profile and the percentage of uEV and tEV in the size range of exosomes (30-100 nm) and microvesicles (100-300 and >300 nm) and concentration of isolated EV from untreated and TNF-α stimulated HUVEC (uEV and tEV, respectively) using different isolation protocols including ExoQ, UCF and SEC.

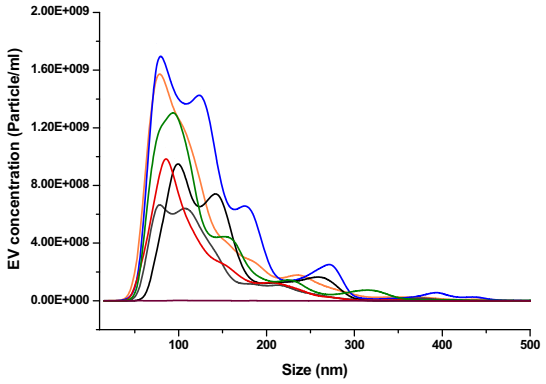

	Exosome % (30-100nm)	Microvesicles % 100-300 nm	>300nm	Mean size (nm)	P value	Concentration (particle/ml)	P Value
uEV- ExoQ	54.4	43.1	2.2	125.5 ± 66.3	0.04*	1.32 ± 0.97 E + 009	0.018**
tEV- ExoQ	41.9	55.5	2.5	137.0 ± 70.2		1.57 ± 0.1 E +009	
uEV- UCF	57.5	41.9	0.49	114.8 ± 54.3	0.12	7.18 ± 0.62 E+008	0.04 **
tEV- UCF	53.1	44.1	2.86	127.9 ± 63.9		1.09 ± 0.07 E+009	
uEV-SEC	48.7	49.8	1.42	125 ± 57.4	0.018*	6.14 ± 0.2 E+008	0.01**
tEV- SEC	35.1	64.8	0.01	138.1 ± 70.8		7.83 ± 0.17 E+008	

*, ** P<0.05 of uEV vs tEV

The data show the means ± SD of three independent replicate measurements. In this test, *P* values <0.05 were considered as statistically significant and they are presented in table at the insert.

from HUVEC. Hence, ELISA was utilized for further confirmation and quantitative measurement of this specific antigen present on EV-surface and in supernatant. In this assay, the specific primary antibody is normally detecting the extracellular domain of ICAM-1, therefore, both soluble and membrane bound isoform of ICAM-1 can be quantified in the conditioned supernatant of HUVEC, and on isolated uEV and tEV. Figure 3 demonstrates that the expression levels of ICAM-1 in the supernatant and EV of all TNF-α stimulated samples were statistically significantly ($P = 0.028$) increased when compared to non-stressed samples. The response of ICAM-1 expression on EV to stress shows a larger range than if measured in the supernatant ($P = 2.6E{-}5$). We also discovered that the concentration of ICAM-1 in the isolated EV is comparable with the supernatant of samples (Figure 3), suggesting that the major part of ICAM-1 in supernatant is transported by EV. The supernatant of cell-free culture mediums supplemented with or without TNF-α served as controls. No significant amount of ICAM-1 was detected in the controls ($P = 0.82$).

Label-free monitoring of antibody-EV interaction on SPR

Finally, SPR was applied for label-free profiling of EV-associated biomarkers. In order to assess the specificity of antibodies toward the EV, we first used an amine coupling procedure to immobilize various antibodies, such as anti-ICAM1, anti-CD63 and anti-rat IgG1 (as a negative control) on the surface of a C1 chip. Antibodies were immobilized onto flow cells with an immobilization level of about 1200 RU (Figure 4, *B*). Next, we analyzed the specific binding activity of each antibody toward EV in a real time manner (Figure 4, *A*). The specific binding responses of isolated uEV for anti-CD63, anti-ICAM-1 and anti-rat IgG1 were 388, 1012 and 76 RU, respectively (Figure 4, *A-B*). These results showed that more tEV bound to anti-ICAM-1 and anti-CD63 when compared to uEV (Figure 4, *A-B*). These results also revealed that isolated EV from stimulated and unstimulated media (uEV and tEV) tended to bind more to anti-ICAM1 than to anti-CD63 (Figure 4, *A-B*).

Convincingly, labeled and unlabeled biomarker based approaches for EV profiling suggested that ICAM-1(+) EV can be a discriminatory diagnostic marker for inflammation-triggered endothelial cells. To explore this further, SPR analyses of patient derived EV with CHD were performed to investigate the potential of ICAM-1(+) EV as prognostic biomarker.

SPR analysis of isolated EV from patient samples with CHD symptoms

The specific interaction of immobilized anti-ICAM-1 toward isolated EV from patient samples with CHD, as well as the

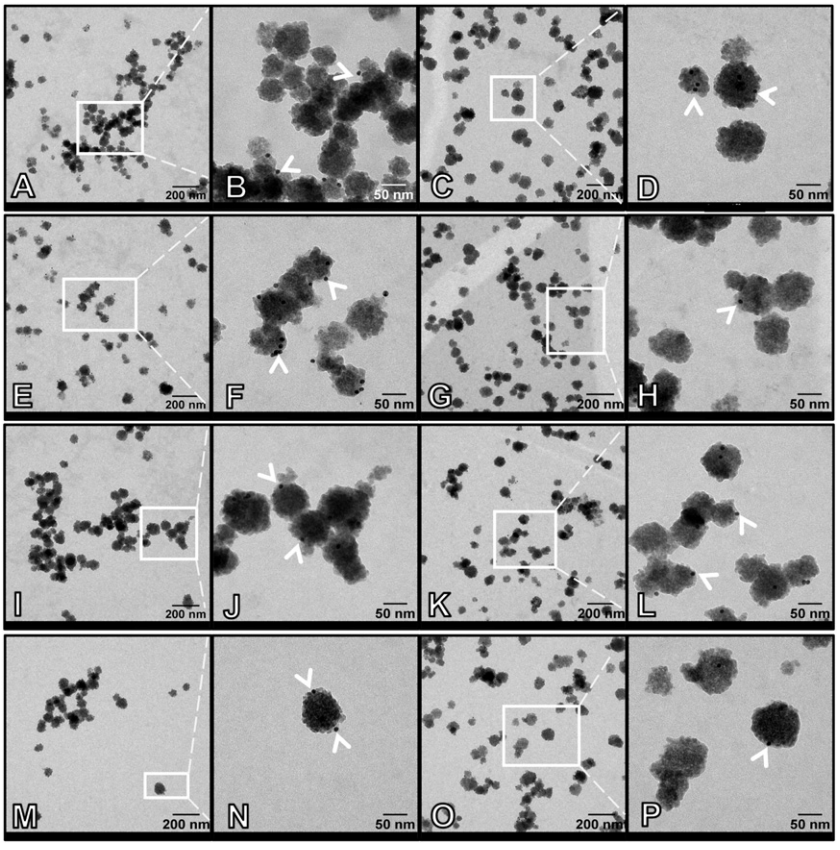

Figure 2. Electron Immunogold labeling micrograph of uEV and tEV isolated from HUVEC using UCF. Antibodies against ICAM-1 (**A-D**), CD9 (**E-H**), CD63 (**I-L**) and CD81 (**M-N**) were used as primary antibodies. 10 nm colloidal gold conjugated goat anti-mouse IgG was applied as secondary antibody in all samples. White arrowheads point toward the gold conjugated goat anti-mouse IgG.

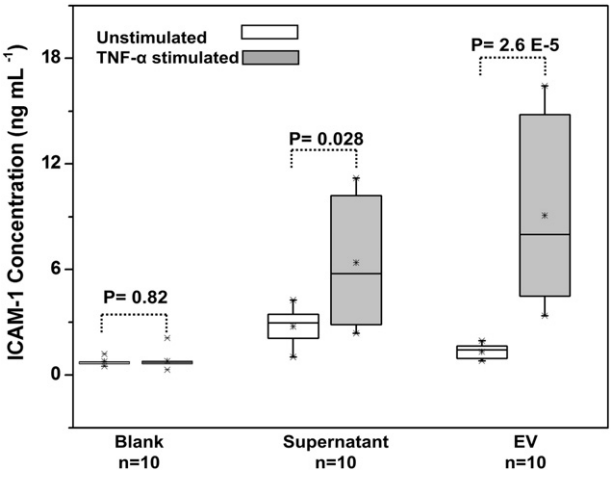

Figure 3. ELISA-based analysis of ICAM-1 content in the supernatant and isolated EV fractions of unstimulated and stimulated HUVEC. The data show the means ± SD of three independent experiments, each consisting of three replicate measurements (n = 9). P values of unstimulated samples *vs* control in the supernatant (P = 0.06) and isolated EV (P = 2.6 E-5) were determined using ANOVA. The supernatant of cell-free culture mediums supplemented with or without TNF-α served as controls. No significant amount of ICAM-1(+) EV was detected in the cell-free controls (P = 0.82).

healthy individuals was monitored using SPR (Figure 4, *C*). Anti-ICAM-1 was captured on four flow cells of C1 chip following an amine coupling procedure as previously described.

Interestingly, EV derived from healthy control persons showed a similar ICAM-1 expression response to TNF-α stimulation as was observed for the HUVEC cells (Figure 4, *A*

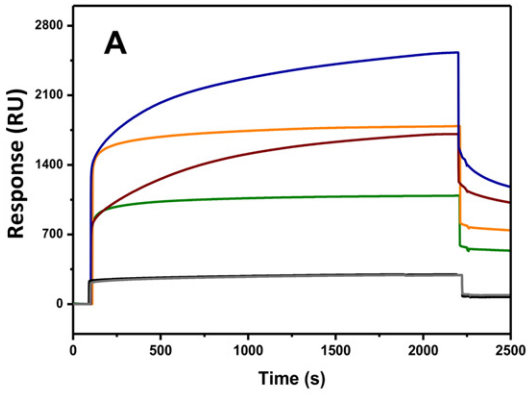

B

Binding interaction (RU)		Immobilization (RU)	
uEV	tEV		
1012 ± 44	1539 ± 323	Anti-ICAM-1	1216 ± 47
388 ± 46	726 ± 125	Anti-CD63	1097 ± 140
76 ± 6	81 ± 12	Anti-IgG1	1169 ± 169

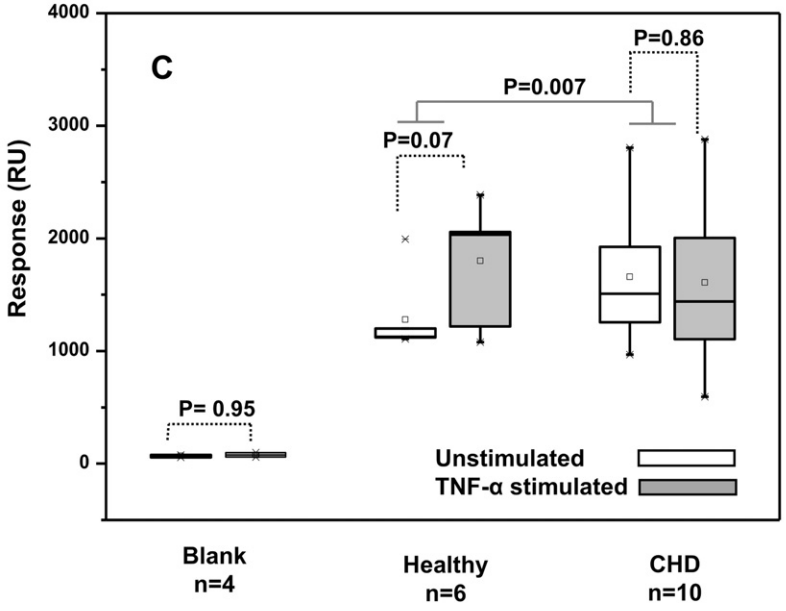

Figure 4. SPR analysis of ICAM-1 and CD63 expression levels on EV. (**A**) SPR profiles of specific binding interaction of uEV and tEV with captured anti-ICAM-1, anti-CD63 and anti-rat IgG (negative control) in real time. (**B**) Response unit of direct covalent capturing of anti-ICAM-1, anti-CD63 and anti-rat IgG1 on biosensor C1 chips ('Immobilization' step) and specific binding interaction of uEV and tEV with the corresponding immobilized antibodies. (**C**) SPR analysis of the binding affinity of captured anti-ICAM-1 on C1 sensor chip towards EVs isolated from the TNF-α stimulated and unstimulated cell-derived supernatant of healthy individuals and patients with CHD. ANOVA was used to analyze the statistical significance between groups of patients and healthy individuals with or without considering TNF-α treatment ($P < 0.05$).

and *C*).TNF-α stimulation of cells increased significantly the level of ICAM-1(+) EV ($P = 0.07$) in the healthy individuals. In contrast, upon stimulation this response was not detected in EV isolated from patients with CHD ($P = 0.86$). Moreover, a higher expression of ICAM-1 was already observed in EV derived from non-stimulated patient cells. Indeed, ICAM-1 expression on EV isolated from patients with CHD was remarkably higher than in healthy controls ($P = 0.007$). However, based on the power analysis of current CHD patient samples and healthy individuals, a minimum number of 60 samples are needed to discriminate between healthy and patient samples without considering the inflammatory stress. These results clearly indicate that the newly developed SPR-based assay can be used for biomarker monitoring in patient samples and subsequently in risk profiling of patients. In future work, our discovered CVD-associated EV biomarker profile will be verified on a large number of patient samples using SPR.

Discussion

Several studies have shown that cardiovascular events are associated with endothelial vascular inflammation which inflicts a cascade of different pathways and eventually results in development of CVD.[18,19] Both EV-counts and EV-content have gained considerable interests as disease-specific biomarkers in diagnosis and prognosis of CVD.[20] Investigating EV directly in body fluids is difficult due to their low abundance of EV. Moreover, the disease-related proteomic and nucleic acid content of EV in body fluid samples are masked by the complex mixture

of all EV present in body fluids. In this regard, we recently established a unique procedure to isolate and culture VEC from patients undergoing percutaneous coronary intervention, and from control persons having catheterization or vascular assessments for different reasons (unpublished data). These unique VEC cultures provide the opportunity to study dedicated subsets of EV in patients and control persons but also allow us to study the impact of external triggers, such as inflammation on these *ex vivo* patient cells.

In this study, the ultrastructural profile of human endothelial cell-derived EV was first optimized on inflammation-induced HUVEC to mimic CVD. So far, HUVECs have been considered as a potential reference model of vascular endothelial cells for the *in vitro* investigation of cellular signaling pathways during the endothelial dysfunction and vascular inflammation associated with CVD.[21] Afterward, discovered CVD associated EV subsets were tested for its applicability on patients suffering from CHD.

For a detailed and reliable molecular profiling and characterization of EV, the isolation of biologically intact EV is essential.[22] In this study, we first characterized the size distribution and the morphology of the isolated EV using three commonly used isolation techniques including UCF, ExoQ and SEC. Our observations are comparable to earlier reported research on EV isolation from cell culture supernatant.[18,22] According to several studies, a greater purity and quantity of intact vesicles can be obtained using the ultracentrifugation method in comparison with other methods.[23] Moreover, ExoQ kit can precipitate and aggregate any other element present in the supernatant.[18] Because of these observations, the biomarker profiling studies in this study were focused on the UCF-based isolated EV.

Several studies have reported that the number of released EV is strictly governed by cellular stress and diseases.[24] An increased number of released EV can indeed be an indication of certain diseases.[9] In our study, the mean size and concentration of tEV isolated using different methods were significantly larger than uEV. An increase in the size of EV can be due to differences in their cargo and the number of membrane-bound proteins. Statistical results are supporting our hypothesis that cellular stress conditions are reflected in the number and the size of secreted EV. Current advances in bio-imaging technology enable the discovery and detection of functional biomarkers. Among the bio-imaging technologies, immunogold labeling with antibodies against known proteins has been applied as a quick, semi-quantitative conventional methodology for exploring the cell-specific antigens and their localization. In this method, the distribution of gold nanoparticles (size ~11 nm) on the outermost layer of EV is proportionally related to the biomarker expression with respect to cellular stress.[17] Membranes of EV are highly enriched in tetraspanins and adhesion protein which are essential for the formation, secretion and maturation of EV. So far, CD9, CD63 and CD81 have been introduced as widely detected tetraspanins biomarkers in cell-derived EV. In addition, during inflammatory responses, the expression of multiple isoforms of adhesion molecules such as ICAM-1 including membrane-bound (mICAM-1) and soluble ICAM-1 (sICAM-1) is upregulated. The sICAM-1 can be produced either independently or by proteolytic cleavage of the membrane-bound form.[25,26] The mICAM-1 is critically contributing in intracellular signaling and to immune and inflammatory responses, as well as potentially enriched in EVs. Therefore, this isoform of ICAM-1 as well as CD9, CD63 and CD81 was our main interest to study. The specific interaction of isolated EV toward antibodies against ICAM-1, CD9, CD63 and CD81 was visualized employing targeted immunogold labeling. We found that the numbers of all ICAM-1(+) and CD63(+) sub-populations of tEV were increased in comparison with their corresponding sub-populations of uEV (Figures 2 and 3). Our observation is in agreement with the findings of Lee et al.[25] They suggested that secreted circulating ICAM-1 from human cells was localized on membrane-like vesicles. They have also demonstrated that ICAM-1(+)-exosomes were shed from TNF-α activated endothelial cells with anti-leukocyte adhesion activity.[25]

Although immunogold labeling and ELISA provide precise and conventional methodologies for exploring and quantifying the cell specific antigens, these label-dependent methods are dealing with extensive sample purification, post-labeling steps and a lack of sensitivity and accuracy in complex media.[11] Therefore, a robust, label-free method is required for the direct detection of the specific EV biomarkers. Nowadays, SPR has drawn a considerable interest as powerful label-free optical biosensor tool for the real-time monitoring of biomolecular interactions.[11] More important, running biomarker binding assays using SPR provides several compelling advantages over label-dependent methods, such as the ability to detect low affinity antibodies or antigens, a calibration-free concentration analysis, the elimination of labels and low sample volume requirements. Other major advantages of SPR are the real-time visualization of specific and non-specific binding interactions, a minimized consumption of materials (μL) and the availability of detailed information about the kinetics of the antigen–antibody interaction when compared to traditional assays. For this purpose, we optimized the SPR methodology for biomarker profiling of EV. We also hypothesized that anti-ICAM-1 and anti-CD63 have the potential to discriminate between EV derived from normal and stressed endothelial cells. Therefore, the specific interaction between captured antibodies and EV was monitored on SPR. The binding of tEV and uEV was higher to anti-ICAM-1 and as compared to anti-CD63. In addition, our results also showed a higher binding of isolated tEV in comparison with uEV. Higher responses and increased binding on SPR chips can be due to the increased number of ICAM-1(+) EV sub-population but can also be explained by a higher expression of ICAM-1 on the surface of individual tEV. The obtained results do confirm our results using immunogold labeling and ELISA methodology. Therefore, biomarker profiling of EV using the SPR tool can provide a novel, fast, label-free and reliable sensing technologies for quantifying EV.[13]

In the optimization phase of this study, we discovered that the elevated level of ICAM-1(+) EV subset is associated with inflammatory stress. A critical step in the initiation and progression of coronary disease is the inflammation-mediated activation of vascular EC, afterward, the upregulation of adhesion proteins such as ICAM, VCAM and E-selectin. These adhesion biomarkers are intimately involved in the recruitment of leucocytes to sites of inflammation, developing atherosclerotic lesions and subsequently development of acute coronary disease.[26] Among these biomarkers, elevated level of

sICAM-1, which has been shed from the cell surface, has been suggested as one of the strong independent predictors of the risk for coronary disease.[26] To our knowledge, there is no report available on the prognostic value of ICAM-1(+) EV subpopulation in patients with CHD symptoms. We demonstrate in this study for the first time the increased release of ICAM-1 carrying EV from EC upon simulation of inflammation by TNF-α using SPR. A significantly higher level of ICAM-1(+) EV isolated from unstimulated and stimulated primary endothelial cells of patients with CHD, as compared to healthy donors was detected. Comparable to the normal HUVEC, TNF-α stimulated cells of healthy persons secreted EV with significant higher ICAM-1 levels as compared to unstimulated cells. These data support the idea that the stage of a disease and the cellular stress conditions in the cell of origin are mirrored in the cargo of the EV produced. Interestingly, we observed that patients at high risk tend to show a different response to TNF-α treatment as compared to control persons. This study can open up novel opportunities for developing a predicting tool to identify a person's risk for CVD using SPR methodology.

Acknowledgments

The authors acknowledge the excellent technical support of An Jacobs (VITO) for NTA measurements. We thank Roland Valcke for using the ultracentrifugation infrastructure.

References

1. Sidney S, Rosamond WD, Howard VJ, Luepker RV. The "Heart disease and stroke statistics—2013 update" and the need for a national cardiovascular surveillance system. *Circulation* 2013;**127**:21-3.
2. Willerson JT, Ridker PM. Inflammation as a cardiovascular risk factor. *Circulation* 2004;**109**:II-2-II-10.
3. Keller S, Sanderson MP, Stoeck A, Altevogt P. Exosomes: from biogenesis and secretion to biological function. *Immunol Lett* 2006;**107**:102-8.
4. Raposo G, Stoorvogel W. Extracellular vesicles: exosomes, microvesicles, and friends. *J Cell Biol* 2013;**200**:373-83.
5. Van der Pol E, Böing AN, Harrison P, Sturk A, Nieuwland R. Classification, functions, and clinical relevance of extracellular vesicles. *Pharmacol Rev* 2012;**64**:676-705.
6. De Jong OG, Verhaar MC, Chen Y, Vader P, Gremmels H, Posthuma G, et al. Cellular stress conditions are reflected in the protein and RNA content of endothelial cell-derived exosomes. *J Extracell Vesicles* 2012;**1**:1-12.
7. Braicu C, Tomuleasa C, Monroig P, Cucuianu A, Berindan-Neagoe I, Calin GA. Exosomes as divine messengers: are they the Hermes of modern molecular oncology? *Cell Death Differ* 2015;**22**:34-45.
8. Zocco D, Ferruzzi P, Cappello F, Kuo WP, Fais S. Extracellular vesicles as shuttles of tumor biomarkers and anti-tumor drugs. *Front Oncol* 2014;**4**:1-7.
9. Lin J, Li J, Huang B, Liu J, Chen X, Chen X-M, et al. Exosomes: novel biomarkers for clinical diagnosis. *Sci World J* 2015;**2015**:1-8.
10. Vlassov AV, Magdaleno S, Setterquist R, Conrad R. Exosomes: current knowledge of their composition, biological functions, and diagnostic and therapeutic potentials. *Biochim Biophys Acta (BBA)* 1820;**2012**:940-8.
11. Im H, Shao H, Park YI, Peterson VM, Castro CM, Weissleder R, et al. Label-free detection and molecular profiling of exosomes with a nano-plasmonic sensor. *Nat Biotechnol* 2014;**32**:490-5.
12. Rupert DLM, Lässer C, Eldh M, Block S, Zhdanov VP, Lotvall JO, et al. Determination of exosome concentration in solution using surface plasmon resonance spectroscopy. *Anal Chem* 2014;**86**:5929-36.
13. Zhu L, Wang K, Cui J, Liu H, Bu X, Ma H, et al. Label-free quantitative detection of tumor-derived Exosomes through surface plasmon resonance imaging. *Anal Chem* 2014;**86**:8857-64.
14. Tadokoro H, Umezu T, Ohyashiki K, Hirano T, Ohyashiki JH. Exosomes derived from hypoxic leukemia cells enhance tube formation in endothelial cells. *J Biol Chem* 2013;**288**:34343-51.
15. Böing AN, van der Pol E, Grootemaat AE, Coumans FAW, Sturk A, Nieuwland R. Single-step isolation of extracellular vesicles by size-exclusion chromatography. *J Extracell Vesicles* 2014;**3**:1-11.
16. Sarker S, Scholz-Romero K, Perez A, Illanes S, Mitchell M, Rice G, et al. Placenta-derived exosomes continuously increase in maternal circulation over the first trimester of pregnancy. *J Transl Med* 2014;**12**:204.
17. Pisitkun T, Shen R-F, Knepper MA. Identification and proteomic profiling of exosomes in human urine. *S A* 2004;**101**:13368-73.
18. Sáenz-Cuesta M, Arbelaiz A, Oregi A, Irizar H, Osorio-Querejeta I, Muñoz-Culla M, et al. Methods for extracellular vesicles isolation in a hospital setting. *Front Immunol* 2015;**6**:50.
19. Sena CM, Pereira AM, Seiça R. Endothelial dysfunction—a major mediator of diabetic vascular disease. *Biochim Biophys Acta (BBA)* 2013;**1832**:2216-31.
20. Bank IEM, Timmers L, Gijsberts CM, Zhang Y-N, Mosterd A, Wang J-W, et al. The diagnostic and prognostic potential of plasma extracellular vesicles for cardiovascular disease. *Expert Rev Mol Diagn* 2015;**15**:1577-88.
21. Onat D, Brillon D, Colombo PC, Schmidt AM. Human vascular endothelial cells: a model system for studying vascular inflammation in diabetes and atherosclerosis. *Curr Diab Rep* 2011;**11**:193-202.
22. Lobb RJ, Becker M, Wen Wen S, Wong CSF, Wiegmans AP, Leimgruber A, et al. Optimized exosome isolation protocol for cell culture supernatant and human plasma. *J Extracell Vesicles* 2015;**4**:1-11.
23. Taylor DD, Gercel-Taylor C. MicroRNA signatures of tumor-derived exosomes as diagnostic biomarkers of ovarian cancer. *Gynecol Oncol* 2008;**110**:13-21.
24. Gardiner C, Shaw M, Hole P, Smith J, Tannetta D, Redman CW, et al. Measurement of refractive index by nanoparticle tracking analysis reveals heterogeneity in extracellular vesicles. *J Extracell Vesicles* 2014;**3**:1-6.
25. Lee HM, Choi E-J, Kim JH, Kim TD, Kim Y-K, Kang C, et al. A membranous form of ICAM-1 on exosomes efficiently blocks leukocyte adhesion to activated endothelial cells. *Biochem Biophys Res Commun* 2010;**397**:251-6.
26. Tanne D, Haim M, Boyko V, Goldbourt U, Reshef T, Matetzky S, et al. Soluble intercellular adhesion molecule-1 and risk of future ischemic stroke: a nested case-control study from the Bezafibrate Infarction Prevention (BIP) study cohort. *Stroke* 2002;**33**:2182-6.